Experimental analysis of real-scale burning tests of artificial fuel packs at the Wildland-Urban Interface

Pascale Vacca [a], Eulàlia Planas [a], Christian Mata [a], Juan Antonio Muñoz [a], Frederic Heymes [b], Elsa Pastor [a,*]

[a] Department of Chemical Engineering, Centre for Technological Risk Studies, Universitat Politècnica de Catalunya·BarcelonaTech, Eduard Maristany 10-14, E-08019 Barcelona, Catalonia, Spain
[b] IMT Mines Alès, 6 avenue de Clavières, 30319 Ales Cedex, France

A B S T R A C T

The combustion of artificial fuels at Wildland-Urban Interface (WUI) homeowner scale has been identified as a contributor to fire spread through a property, often leading to the ignition of structures, hence involving major safety issues at community level. However, little information on the real-scale burning behaviour of these type of fuels is available. These fuels are usually located close to the main structure of a property and are often piled together, forming packs containing different types of materials. Real-scale tests on four different fuel packs have been performed to gather quantitative data on items that are commonly present on WUI properties. The fuel packs consisted of typical combustible materials present in porches, gardens, backyards or stored in secondary structures. Data on Heat Release Rate (HRR), Mass Loss Rate, fire load, smoke species concentration, heat flux, temperature and flame height are provided. The duration of the fires was between 49 and 83 min. Peak HRR values between 383 kW and 2.55 MW were recorded, along with flame heights up to 3.6 m. Radiative heat fluxes were calculated for each test, and safe distances for people were identified. Reported data can be used to quantify vulnerabilities of WUI properties through Performance-Based Design methodologies. Results show that the most hazardous fuel packs out of the four tested are those containing pallets, cardboard, paint, foam mats and garden furniture. In all cases, the flaming area expanded significantly increasing the risk of fire spread through a property even after the passage of the wildfire front.

Keywords:
WUI fires
Heat release rate
Flame geometry
Combustion
Safety distances

1. Introduction

Fires in Wildland-Urban Interface (WUI) communities have rapidly expanded in frequency and severity over the past few decades, and the number of structures lost per year has increased significantly (Caton et al., 2017). When residential developments are exposed to extreme wildfire conditions numerous houses can ignite and burn simultaneously, overwhelming firefighters and reducing fire protection effectiveness (Cohen, 2008; Ronchi et al., 2019). This has led to the need for self-protection and therefore to the creation of fire-adapted communities which can safely co-exist with wildfires (Vacca et al., 2020).

The ignitability and integrity of a home are issues of the so-called WUI microscale (Pastor et al., 2019; Scarponi et al., 2020), which includes a home and its immediate surroundings and is thus an extended concept of the Home Ignition Zone (Cohen, 2008; Mell et al., 2010). During wildfires, fire impact at this scale depends mainly on the characteristics of the home and of its nearest surroundings (Cohen, 2000).

The WUI microscale is characterized by the presence of natural fuels, such as ornamental vegetation and ground fuels, and artificial fuels, such as outdoor furniture and stored materials, which are located in the home's surrounding environment. These elements can be ignited by firebrands generated by the main fire front or by nearby burning structures or materials (Pastor et al., 2019), as well as by radiant exposure or direct flame contact, if the defensible space around the property is not sufficient (Caton et al., 2017). They can therefore contribute to the propagation of the fire through a urban settlement (Manzello et al., 2018). These fuels have the potential to burn with significant intensity and duration, possibly putting homes at risk of ignition and structural failure, should they be located close enough to affect their weakest elements (e.g. glazing systems, poorly maintained vents, etc.).

* Corresponding author.
E-mail address: elsa.pastor@upc.edu (E. Pastor).

Fig. 1. A garage exposed to the passage of the fire in Mati (Greece, 2018).

Fig. 2. Warehouses with materials completely destroyed in the Monchique fire (Portugal, 2018).

Preventive actions at the immediate surroundings of the house must thus be adopted to guarantee structure integrity and create self-defensible spaces. Considering home and site characteristics when designing, building, siting, and maintaining a property can reduce WUI fire losses (Cohen, 2000). There is a need for research on defensible space, to quantify the effectiveness of current recommendations and to standardize the guidelines for defensible space across wildland fire-prone areas (Hakes et al., 2017; Ricci et al., 2021). A WUI-specific Performance-Based Design methodology, which is currently being developed, is a suitable and promising approach to analyze fire impact at the microscale (Vacca et al., 2020). For this purpose, quantitative information on the fuels that can be present on a property is needed, so that the role of these fuels in a home's ignition process can be defined and characterized. This will allow for a more accurate assessment of WUI microscale vulnerabilities. The burning behaviour of common fuels that can be found indoor (e.g. pieces of furniture and small appliances) has been extensively analysed in small- and real-scale tests (Hurley et al., 2016; National Fire Research Laboratory, 2020), however, there is a lack of quantitative data on the burning behaviour of artificial fuels and fuel packs that are frequently located in the surroundings of WUI structures. The hazard associated to these fuel packs is given for example by the large heat accumulation due to their ignition in semi-confined spaces (Fig. 1 and Fig. 2, Caballero and Sjöström, 2019), which can lead to fire spread through a property due to the ignition of other surrounding elements (Vacca et al., 2020). This hazard is currently poorly characterized (Mell et al., 2010) and it has been observed to be an accident scaling factor in recent WUI fire events (Vacca et al., 2020; Manzello et al., 2018).

Experiments consisting of the combustion of four different fuel packs have been performed during the WUIVIEW project (ECHO/2018/826522). All four fuel packs contain items commonly found on WUI properties, and they correspond to residential fuel scenarios identified from past fires (Caballero and Sjöström, 2019).

The objective of these real-scale tests is to obtain quantitative information on the fire hazard of typical artificial fuel packs present at the WUI microscale. The new acquired data can serve as input for WUI Performance Based Design evaluations in order to obtain quantitative results for the assessment of WUI microscale vulnerabilities, with the use of tools such as Computational Fluid Dynamics (CFD) modelling. This information can also be of interest to firefighters that deal with WUI fires, for the assessment of hazards when working on a property containing these types of fuels. Furthermore, the outcome data on microscale vulnerabilities could provide useful dissemination material in civil protection campaigns designed to rise risk awareness amongst WUI communities.

2. Methods and materials

The tests were performed in the large scale testing platform of the The French National Institute for Industrial Environment and Risks (INERIS), equipped with a Tewarson calorimeter with a capacity up to 10 MW. The facility consisted of a 10mx10m room with a 5mx5m scale, which was covered by sand, on which the items were placed. The hood was located directly above the scale, and air could flow in the room through two openings located on the northern and southern sides of the room. Ambient temperature was around 7 °C for the first two tests, 6 °C for the third and 9 °C for the final test.

The instrumentation used in the tests is given in Fig. 3. Medtherm Gardon heat flux sensors were located in the same position for each test. Meters F1, F2, F5 and F6 measured the total heat flux at a height of 1 m, meters F3 and F7 at a height of 2 m, and meter F4 at 2.5 m. Five visual cameras recorded the tests for the identification of their timeline, while an infrared camera (Optris PI-640) recorded flame temperatures. Flame heights and width could also be extracted from the recordings of the IR camera located on the north side of the facility. This was performed with the aid of a software that allows to segment video sequences, extracting a mask of the flame contour from several IR-images, as given in Table 6 (Mata et al., 2018). The highest and lowest pixel of the flame are detected automatically (shown by the yellow and red dots in Fig. 17). The segmentation process is based on Chan Vese Active Contours without edges (Chan and Vese, 1999) using a set of iterations. The distance between the pixels (blue and red dots in Fig. 17) can be obtained in meters by performing a resolution calculation based on a reference image from the IR camera. This way flame height and fire width could be calculated for each frame.

Six type K 1.5 mm thermocouples (T1-T6) were located on the fuel pack items to record flame temperatures. The recording system however malfunctioned during tests 2 and 4, so data from these thermocouples was only obtained for tests 1 and 3. Eight 1 mm thermocouples (T7-T14) were placed at certain distances from the burning fuel pack to record air temperatures at a height of 60 cm. The distance between these eight thermocouples and the fuel packs was different for each test, as can be seen from Table 1, due to the different sizes of the packs. Thermocouple T13 did not record any data for test 2 due to malfunction.

Heat Release Rate (HRR), mass loss, smoke's species concentration, heat flux (kW/m^2) and temperature (°C) data was recorded every two seconds. Two gas burners were used for the ignition of the items, which provided a HRR up to 140 kW and were turned off once the items showed self-sustained flaming, given that the goal of the tests was to determine their burning behaviour once ignited, and not their critical values for ignition. The tests were performed in well-ventilated

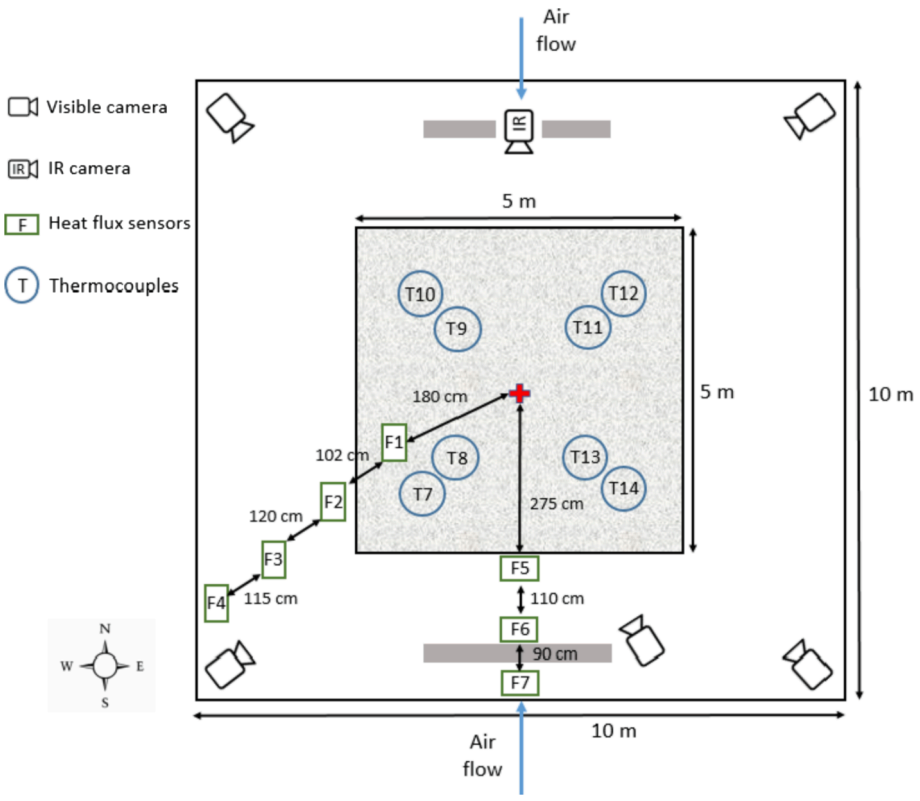

Fig. 3. Experimental setup. The grey rectangles indicate stacks of bricks behind which observers were standing. The red cross indicates the middle of the 5x5 m^2 platform. (For interpretation of the references to colour in this figure legend, the reader is referred to the web version of this article.)

Table 1
Location of thermocouples measuring air temperatures.

Thermocouple	Distance from the fuel pack [m]			
	Test 1	Test 2	Test 3	Test 4
T7	1.10	1.21	1.11	1.10
T8	0.60	0.71	0.61	0.60
T9	1.02	1.55	0.74	0.72
T10	1.52	2.05	1.24	1.22
T11	0.52	0.74	0.60	0.55
T12	1.02	1.24	1.10	1.05
T13	0.57	–	0.36	0.60
T14	1.07	0.98	0.86	1.10

conditions. Smoke species concentrations were measured from the exhaust flow. CO_2 and CO concentrations were given by a Non-Dispersive Infrared (NDIR) analyzer, the total unburned hydrocarbons (THC) concentrations were measured by a Flame Ionization Detector (FID), and O_2 concentrations by a paramagnetic oxygen analyzer.

The first fuel pack consisted of outdoor children toys, bags with clothes and boxes with paper and books, the second one of pallets, cardboard sheets, paint buckets and foam mats. The fuels in the third test were an outdoor table with six chairs, six cushions and a parasol, and those in the final test consisted of three oil-based paint buckets. Items' dimensions, weight and material composition for each test are given in Table 2.

2.1. Test 1 - outdoor toys, clothes, books and paper

The fuel pack in this test consisted of fuels that could be found together in backyards or stored in secondary structures at the WUI. These comprised plastic toys, 3 bags of clothes (one containing cotton, one wool and one synthetic fabrics) and 2 boxes containing books and paper (Fig. 4). The total mass of the fuel pack amounted to about 69 kg. The two burners pointed towards opposite sides of the fuel pack, one towards the slide and the other towards the back of the toy house, and were active for 70 s. By this time, the toy house had partially melted and its roof had collapsed on top of the items placed in the house. After 3 min all plastic items had completely melted, creating a pool fire scenario.

Thermocouple T1 was placed on top of the toy house, T2 inside the bag containing cotton clothes, T3 inside the bag of synthetic clothes, T4 inside one of the boxes, T5 inside the bag containing wool clothes and T6 at the bottom of the house. The other thermocouples were placed according to the distances given in Table 1.

2.2. Test 2 - Pallets, foam mats, cardboard and paint

Test 2 consisted of a fuel pack containing typical fuels that are stored in semi-confined spaces located on WUI properties. These are 3 pallets, 4 small mattresses, 11 cardboard sheets, and 7 plastic buckets containing each 12 l of oil-based paint (Fig. 5). The items' characteristics are given in Table 2 and the total weight of the fuel pack amounted to 140.8 kg. The two burners were placed on opposite sides of the fuel pack, pointing towards the stack of pallets, and were active for about 30 s, during which nearly all items ignited, with the exception of the cardboard sheets shielded from the flames. The paint started spilling from the buckets after about 40 s, creating a pool underneath the pallets and the cardboard. The foam mats melted on top of the pallets after 70 s. By this time all items of the fuel pack had ignited.

In test 2 thermocouples registering air temperature were placed around the fuel pack as given in Table 1.

2.3. Test 3 - Table and chairs

The third fuel pack represents a typical outdoor furniture set present in gardens or porches, usually located in the vicinity of a WUI dwelling. It consisted of an outdoor table with 6 chairs, 6 cushions and 1 parasol,

Table 2
Item characteristics for each test. Test 4 contains the same paint buckets as those in test 2.

Item	Length [m]	Width [m]	Height [m]	Mass [kg]	Material
Test 1					
Toy house	1.08	1.40	1.15	13.9	Polypropylene
Slide	1.35	0.46	0.67	3.32	Polyethylene
Cotton clothes bag	0.60	0.60	0.80	10.7	Cotton, polyethylene
Wool clothes bag	0.60	0.60	0.80	3.4	Wool, polyethylene
Synthetic clothes bag	0.60	0.60	0.80	3.8	Polyamide, polyester, polyethylene
Toy lawn mower	0.60	0.23	0.25	0.36	Polypropylene
Tricycle	0.52	0.68	0.52	3.4[a]	Polypropylene, steel
Painting	0.90	0.60	0.03	1.4	Wood, paper, paint
Box with books	0.30	0.40	0.30	13.48	Paper, cardboard
Box with paper	0.30	0.40	0.30	14.76	Paper, cardboard
Box of tricycle	0.47	0.22	0.46	0.2	Cardboard
Test 2					
Pallet 1	1.2	0.8	0.13	11.4	Wood
Pallet 2				13.2	
Pallet 3				15.7	
Foam mat	1.2	0.6	0.12	2.15	Polyester
Cardboard	1.6	0.004	0.65	0.55	Cardboard
Paint bucket	0.28	0.28	0.22	12.27	Oil-based paint Polypropylene bucket
Test 3					
Table	2.20	1.00	0.72	23.00	Polypropylene
Chair	0.58	0.59	0.91	2.72	Polypropylene
Cushion	0.38	0.38	0.02	0.07	Cotton, polyester
Parasol	3.00	3.00	2.50	11.50[b]	Polyester, steel

[a] including 1.4 kg of steel
[b] including 8.25 kg of steel

as can be seen in Fig. 6. The dimensions, weight and material composition of the items are given in Table 2. The total weight of the fuel pack amounted to 51.3 kg. The two burners were directed towards each end of the table, pointing underneath the table towards the back of the chairs. The table and chairs started melting within 20 s from the activation of the burners, and within 1 min, four chairs had collapsed to the ground. During this test the two burners malfunctioned and did not flare in a continuous way, providing effective ignition for a total of about 1.5 min. They were then stopped after 130 s from the start of the test. Within 4 min all the items had melted creating a pool fire scenario, which burned until the stop of the test, after 49 min.

In this test, five thermocouples (T1, T2, T3, T5, T6) were placed on five chairs, T4 was placed on the table underneath a cushion, while the other eight were placed further from the fuel pack, at the distances given in Table 1.

2.4. Test 4 – Paint buckets

Test 4 consisted of 3 plastic buckets containing each 12 l of oil-based paint (Fig. 7), which are typical fuels that are stored on properties at the WUI. These buckets had the same characteristics as those present in test 2. The total weight of this fuel pack amounted to 36.8 kg. Only one burner, pointing towards the middle bucket, was used to ignite the items for 35 s. Within 45 s from the start of the test all three buckets had partially melted and released the paint onto the floor, creating a pool fire scenario. After 85 s all the buckets had completely melted.

In this test, the thermocouples were located at different distances from the fuel pack, as given in Table 1.

3. Results and discussion

As previously mentioned, the combustion of the fuel packs in test 1, test 3 and test 4 created pool fire scenarios, due to the presence of a high amount of plastic materials. This did not happen in test 2, which mostly consisted of cellulosic materials. HRR, MLR, fire load, smoke species concentrations, heat fluxes, temperatures and flame heights have been obtained for each test. Peak values are given in Table 3, while details are discussed in the following sections.

3.1. Heat Release Rate, growth rate, mass loss rate and fire load

Heat Release Rates were recorded for each test as given in Fig. 8. The HRR measured for each fuel pack also includes the one of the burners, which is considered as negligible given the fact that the maximum operational time of the burners is 1.5 min, corresponding to a HRR of 140 kW, and that for test 3 the operational time was discontinuous. Tests 3 and 4 were stopped once the fire had extinguished, while tests 1 and 2 ran until the HRR values dropped below 45 kW.

For all test the peak HRR values are reached within the first 5 min. The fuel pack of test 2 presented the highest HRR values, reaching a peak of 2.55 MW, while the one of test 4 resulted in much lower HRR values, not even reaching 400 kW.

The fire growth rate of the different fuel packs indicates how fast a fire will reach its peak HRR and can be calculated with Equation (1) (Heskestad, 1982).

$$\alpha = Q_{peak}/t^2 \quad (1)$$

The fuel pack of test 2, which is the one that contained the most cellulosic materials, had a fire growth of 0.077 kW/s^2, which is between a fast and ultra-fast growth (National Fire Protection Association, 1985). Tests 1 and 3 showed a similar fire growth, of respectively 0.026 kW/s^2 and 0.023 kW/s^2, between medium and fast. These are the fuel packs with the most plastic materials. The paint in test 4 had the lowest fire growth, of 0.015 kW/s^2, closer to a medium one.

The mass loss and the Mass Loss Rates (MLR) averaged over time were recorded as given in Fig. 9 and Fig. 10 respectively. The most significant mass loss happened for all tests during the first 500 s, and the third fuel pack showed the most substantial mass loss during this time. When the tests were stopped, the fuel packs lost 63%, 52%, 65% and 21% in tests 1, 2, 3 and 4 respectively (excluding the non-combustible materials present in fuel packs 1 and 3).

As for the HRR, the fuel pack in test 2 showed higher MLR peak values (Fig. 10b). The fuel pack in test 4 showed much lower values (Fig. 10d), which are reflected in the much lower HRR curve.

Because the combustion under natural fire conditions is usually incomplete, the effective contribution of the fire load to the energy released during a fire is smaller than the total fire load (Fontana et al.,

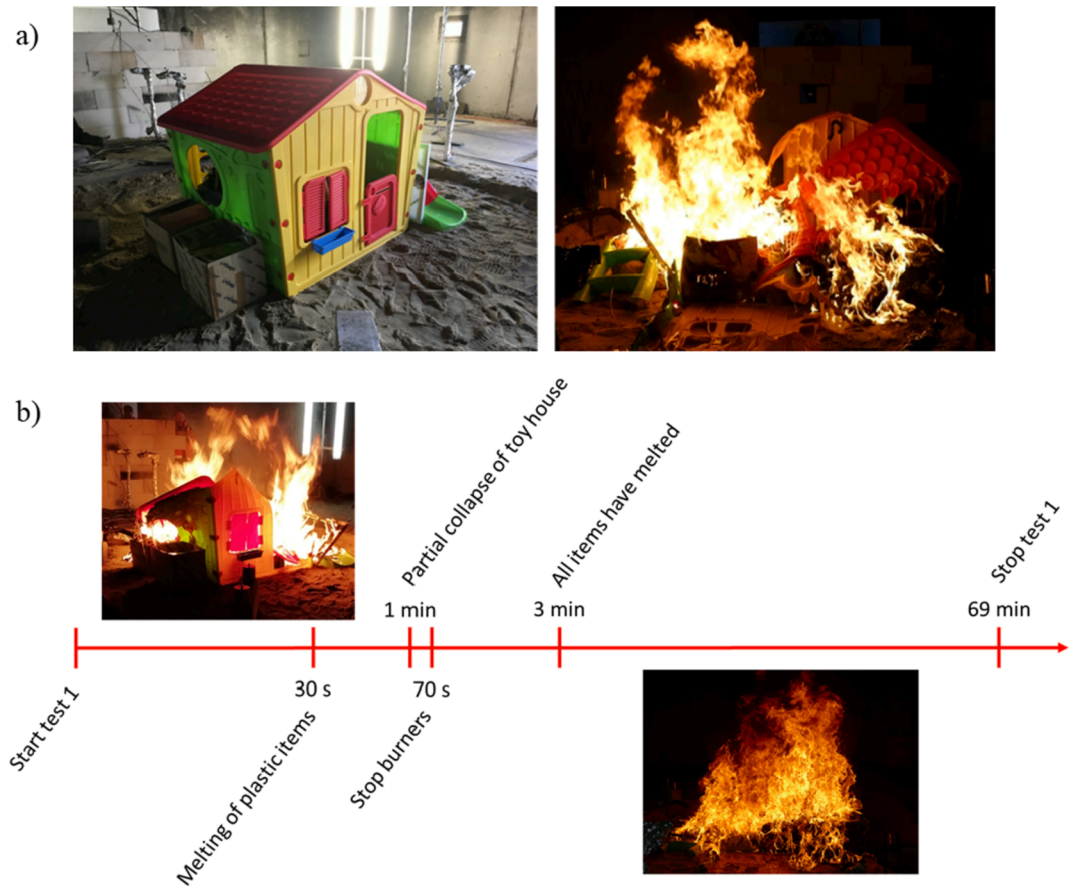

Fig. 4. Test 1. a) on the left: fuel pack just before ignition, on the right: fuel pack burning 90 s after ignition; b) timeline of the test.

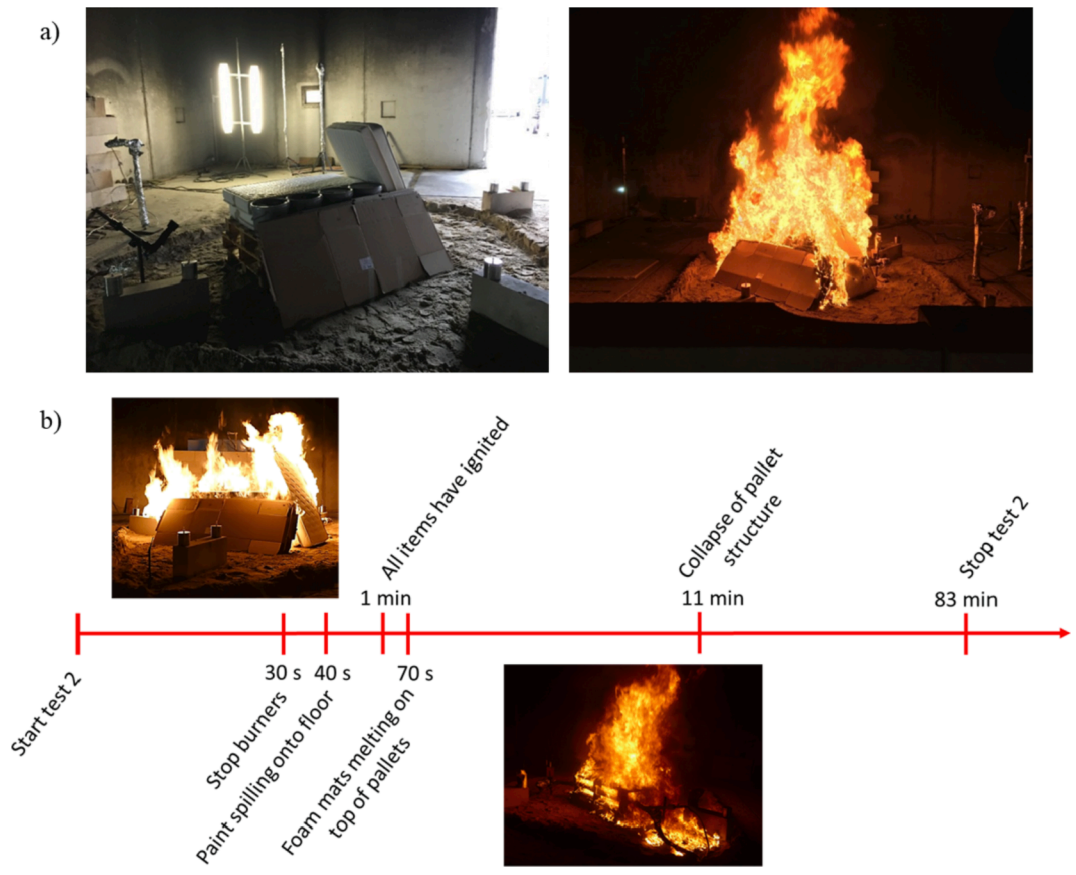

Fig. 5. Test 2. a) on the left: fuel pack just before ignition, on the right: fuel pack burning 90 s after ignition; b) timeline of the test.

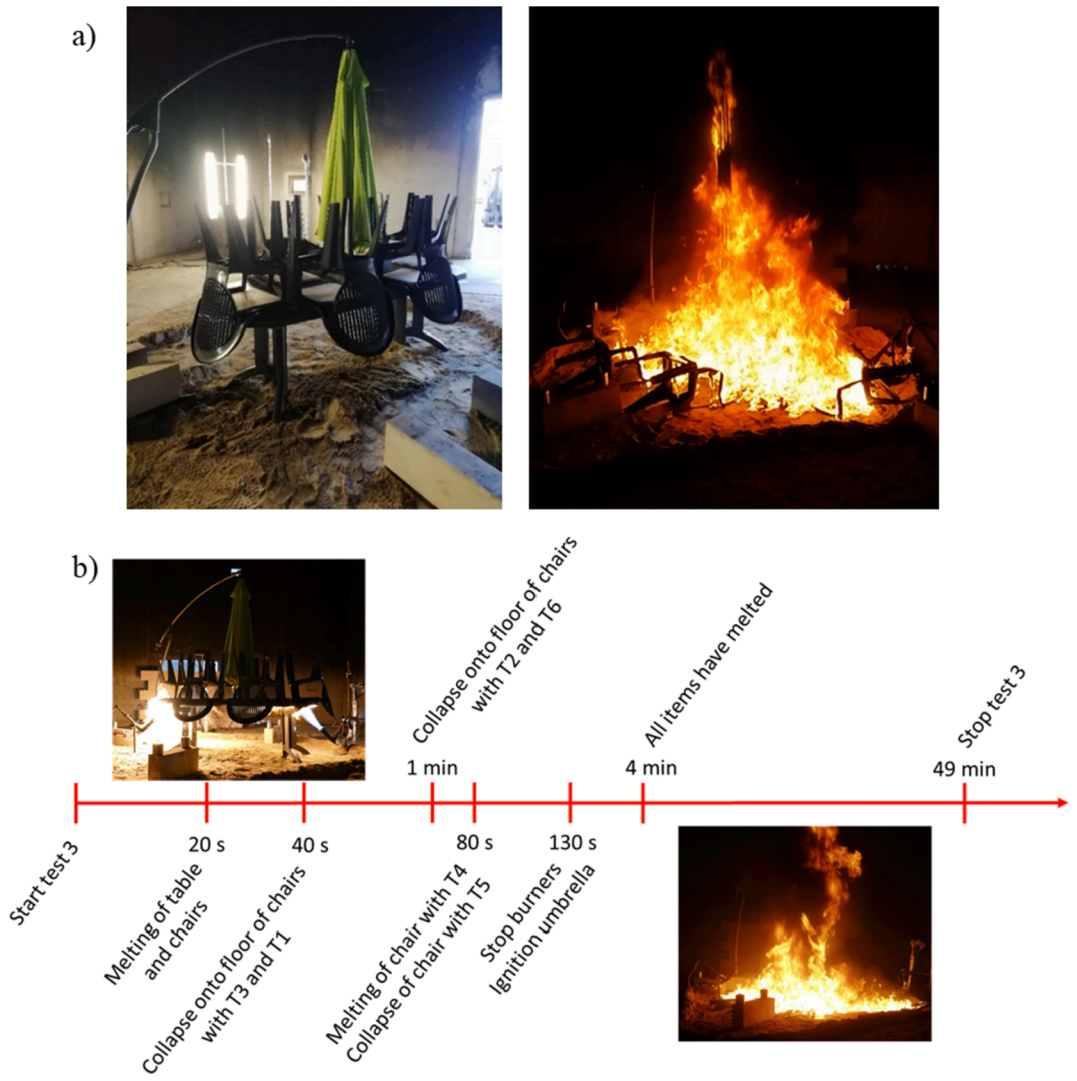

Fig. 6. Test 3. a) On the left: fuel pack just before ignition, on the right: fuel pack burning 150 s after ignition; b) timeline for the test.

2016). The effective fire load for each test, calculated by integrating the HRR curves, is given in Table 3. The fuel pack reaching the highest HRR value is also the one with the highest effective fire load. The fire load of test 1 is higher than the one of test 3, which presented a higher HRR peak value but a shorter fire duration.

3.2. Species concentrations

Oxygen (O_2), carbon dioxide (CO_2), carbon monoxide (CO) and the total unburned hydrocarbons (THC) concentrations were measured in the exhaust duct (Fig. 11). For all fuel packs, the concentration of CO_2 remained well below 5%, and the one of O_2 always above 19%. The fuel pack that produced the highest CO_2 concentration is that of test 2, reaching 1.3%. Test 2 also reached the highest CO and THC concentrations, at 193 ppm and 89 ppm respectively. Average CO_2 and CO yields (amount generated per unit mass of burned fuel) calculated for each test are given in Table 4. The fuel pack in test 3 provided the highest average CO_2 yield, while the highest average CO yield was found for the fuel pack of test 1. The fuel packs containing a bigger variety of materials (tests 1 and 2) are those which present higher average CO yields. CO_2/CO ratios are between 118/1 and 67/1, indicating an efficient combustion (Hurley et al., 2016).

3.3. Heat fluxes

The recorded total heat fluxes for each test are given in Fig. 12. The peak heat fluxes were recorded by meters F1 and F5, which were located the closest to the fire at a distance of approximately 1.5 m for tests 1 and 4, 2 m for test 2 and 1.3 m for test 3, at the lowest measuring height. For all tests, peak heat fluxes were registered before the fire reached its peak HRR, but at instants when the burners had already been switched off. This depends on the fact that the items located the closest to the heat flux sensors were reaching their peak HRR when other items had not yet done so. The highest heat fluxes were recorded for test 2 and test 3 as respectively 19.91 kW/m^2 by F5 (located approximately 2 m from the fuel pack) and 21.05 kW/m^2 by F1 (located approximately 1.3 m from the fuel pack). The peak heat flux value for test 1 was recorded as 11.38 kW/m^2, and the one for test 4 as 4.31 kW/m^2.

The radiative heat flux from the flames is calculated with the following equation at the time when the peak total heat flux was recorded (Janssens, 2016):

$$\dot{q}_f'' = \varphi \varepsilon_f \sigma T_f^4 \quad (2)$$

The emissivity of the flame ε_f is assumed to be 1, since the flame is assumed to be a cylindrical, blackbody homogeneous radiator, σ is the Stefan-Boltzmann constant, T_f is the flame temperature and the view factor φ is calculated according to Equation 3 (Shokri and Beyler, 1989):

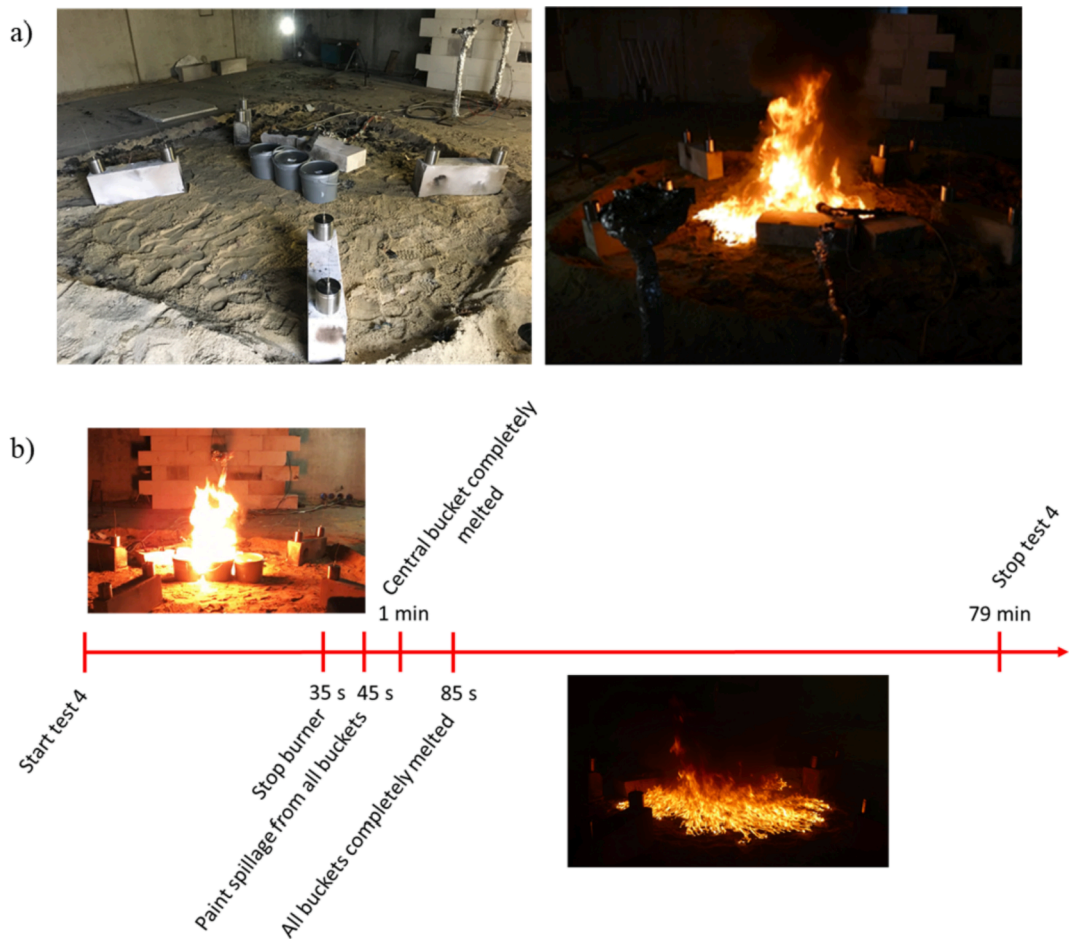

Fig. 7. Test 4. a) On the left: fuel pack just before ignition, on the right: fuel pack burning 70 s after ignition; b) timeline for the test.

Table 3
Peak values recorded for each test.

Peak values	Test 1	Test 2	Test 3	Test 4
Initial mass [kg]	69.0	140.8	51.3	36.8
HRR [kW]	1472	2551	2178	383
MLR [kg/s]	0.20	0.30	0.25	0.15
CO concentration [ppm]	73.2	192.8	160.9	62.8
Flame height [m]	2.65	3.23	3.60	2.64
Air temperature [°C]	76	104	148	115
Heat flux [kW/m^2]	11.4	19.9	21.1	4.3
Fire duration [min]	69	82	49	72
Effective fire load [MJ]	1121	1743	1008	313

$$\varphi=\frac{1}{\pi S}tan^{-1}\left(\frac{h}{\sqrt{S^2-1}}\right)-\frac{h}{\pi S}tan^{-1}\sqrt{\frac{(S-1)}{(S+1)}}+\frac{Ah}{\pi S\sqrt{A^2-1}}tan^{-1}\sqrt{\frac{(A+1)(S-1)}{(A-1)(S+1)}}$$

$$\text{with}=\frac{2L}{D};h=\frac{2H}{D};A=\frac{(h^2+S^2+1)}{2S} \quad (3)$$

L is the distance between the centre of the cylinder and the target, D is the diameter of the fire, and H is the flame height. Table 5 gives the values used to calculate the radiative heat flux for each test 1.5 m from the burning fuel pack. The values of the flame temperature and height are those recorded by the IR camera at the instant when the peak total heat flux was recorded.

3.4. Temperatures

The temperature profiles registered by the thermocouples in test 1 are given in Fig. 13. A peak fire temperature of 931 °C was recorded by T2, located inside the bag containing cotton clothes (Fig. 13a). T5, located in the bag of clothes under the slide, registered temperatures above 500 °C for the majority of the duration of the fire. The highest air temperatures were registered by T8 and T11, located on the opposite sides of the fuel pack, at respectively 76 °C at 232 s and 67 °C at 120 s (Fig. 13b).

For test 2, only air temperatures were recorded by the thermocouples, as given in Fig. 14. The highest temperatures were recorded by T8 and T14, with peaks of respectively 104 °C at 74 s and 103 °C at 122 s. These peaks were registered before the HRR reached its peak value. The IR camera recorded flame temperatures greater than 900 °C, with an emissivity of 1 (results not shown).

The temperature profiles registered by the thermocouples in test 3 are given in Fig. 15. A peak temperature of 964 °C is recorded by T2, located on the back of one of the chairs, at 162 s. At this time both the chair and the table had collapsed and were melting. The highest air temperature values were recorded by T8, with a peak of 148 °C at 262 s. Temperature peaks are registered around the time the fire reaches its peak HRR values, with the exception of those registered by T1, which reaches a peak temperature of 743 °C at 666 s. This delay is caused by the fact that the chair to which the thermocouple was attached to collapsed further from the table and thus melted at a later stage.

In the final test, only air temperatures were recorded by thermocouples (Fig. 16). Peak temperatures were given by T8 as 115 °C at 394 s and by T13 as 99 °C at 162 s (when the peak HRR is recorded). The thermocouples were placed on the side of the burner, thus on the side where the buckets melted first, releasing most of their content towards them. The IR camera recorded flame temperatures greater than 900 °C (results not shown).

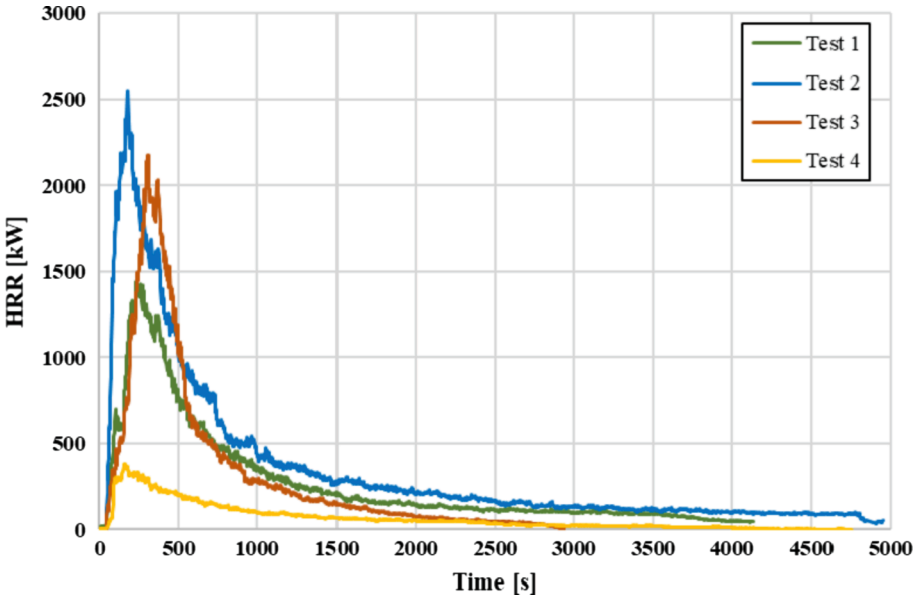

Fig. 8. Heat Release Rates.

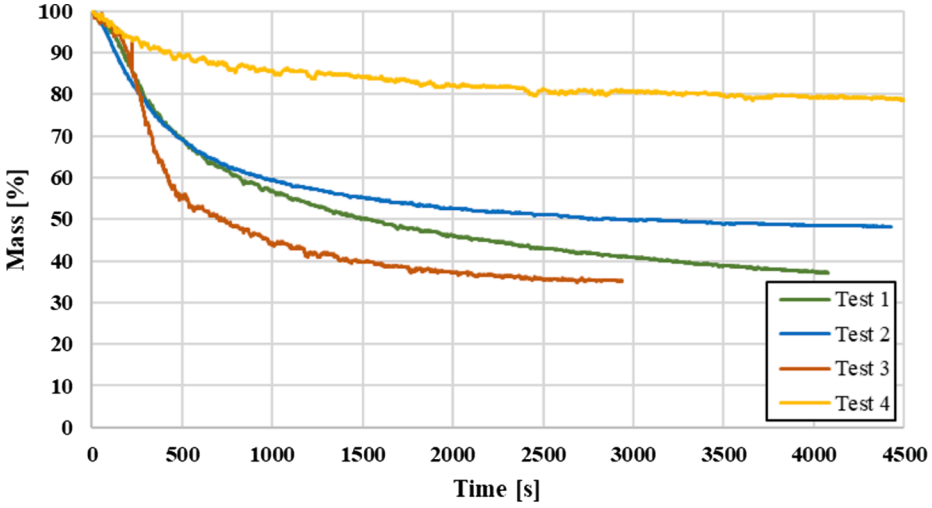

Fig. 9. Mass loss progression over time for each test.

For all tests, thermocouple T8 registered the highest air temperature values at distances between 0.6 and 0.71 m from the fuel packs. The distance between the flaming source and the thermocouples was however reduced during tests 1, 3 and 4, since they resulted in pool fire scenarios and the fuel reached the base of the stand of the thermocouple. For test 2 this distance remained unchanged.

3.5. *Flame height and fire width analysis*

Fig. 17 shows an example for each test of an IR frame corresponding to an original image in the left (a); the segmented image is shown in the middle (b), and finally an example of the measurement of the flame height is depicted in the last image (c).

A description of the obtained results for each test is depicted in Table 6. The average flame height was recorded for the first 32 min for test 1, 20 min for tests 2 and 3, and 29 min for test 4. After these times, flame height had significantly reduced.

Flame heights averaged every 6 s are given in Fig. 18. Peak flame heights were recorded before the fire reached its peak HRR for all tests. Tests 1, 2 and 3 showed a sudden drop in flame height of approximately 0.8 m at 505 s, 600 s and 400 s respectively. Before these instants, the average flame height is 1.82 m for test 1, 2.13 m for test 2 and 2.69 m for test 3. Afterwards the average dropped down to 0.71 m, 0.89 m and 0.78 m. Tests 4 showed a more gradual flame height decrease over the course of time.

The same methodology was applied to obtain the maximum width of the fire, which is 4.32 m for test 1, 4.01 m for test 2, 4.40 m for test 3 (Fig. 19), and 1.57 m for test 4. Considering a circular fire, an approximate peak Heat Release Rate Per Unit Area (HRRPUA) can be calculated for each fuel pack based on these values, which results in 100.4 kW/m^2 for test 1, 202.0 kW/m^2 for test 2, 143.2 kW/m^2 for test 3 and 197.8 kW/m^2 for test 4.

3.6. *Discussion of the results*

The fuel packs that gave the highest values, and are therefore considered the most hazardous out of the four, are the one in test 2 (pallets, cardboard, paint buckets and foam mats) and the one in test 3 (table, chairs, pillows and parasol). The fuel pack of test 2, with the highest HRR and HRRPUA, is also the one with the highest mass.

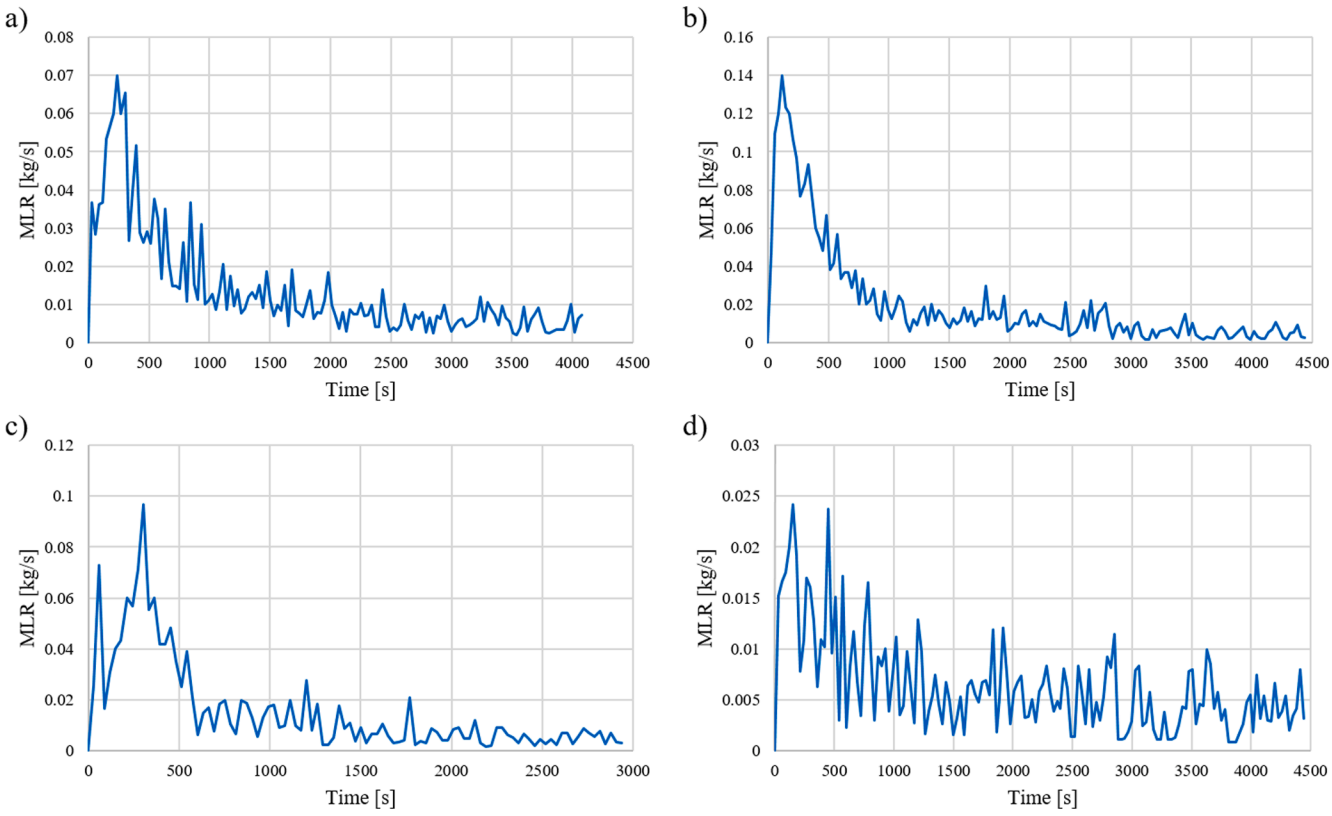

Fig. 10. Mass Loss Rate averaged every 30 s for: a) test 1, b) test 2, c) test 3 and c) test 4.

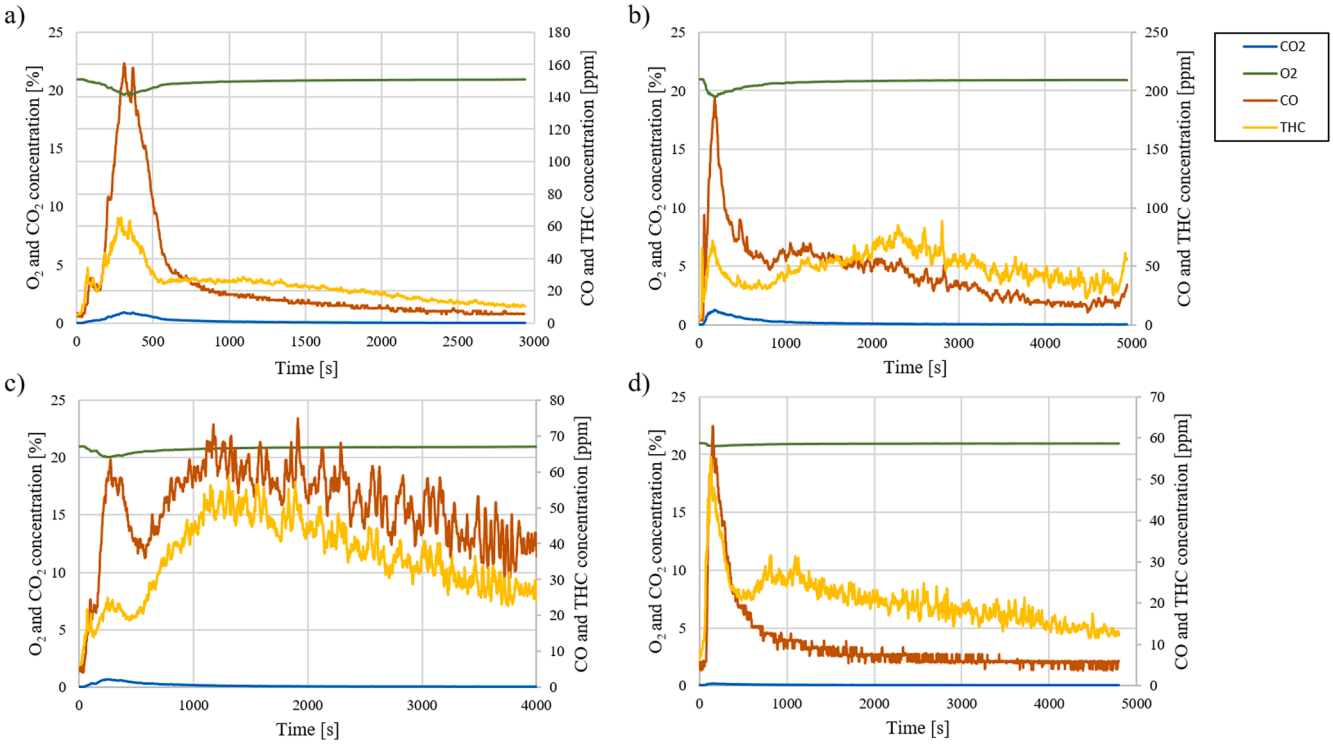

Fig. 11. Species concentrations for: a) test 1, b) test 2, c) test 3 and d) test 4.

However, those of tests 1 and 3 do not follow this trend: test 3 has a lower mass than test 1, but a higher HRR and HRRPUA. This suggests that the total mass of fuel packs cannot be used as an indicator of the risk they pose in case of combustion, but a calculation of their approximate gross heat content can be useful. This can be calculated for each fuel pack taking into account the mass of each item and the gross heat of combustion of the materials composing the item. The items made out of polypropylene (e.g. table, chairs, toy house) and the oil-based paint

Table 4
Average CO_2 and CO yields.

Yield [kg/kg]	Test 1	Test 2	Test 3	Test 4
Y_{CO_2}	2.10	2.63	2.73	2.56
Y_{CO}	0.07	0.06	0.02	0.02

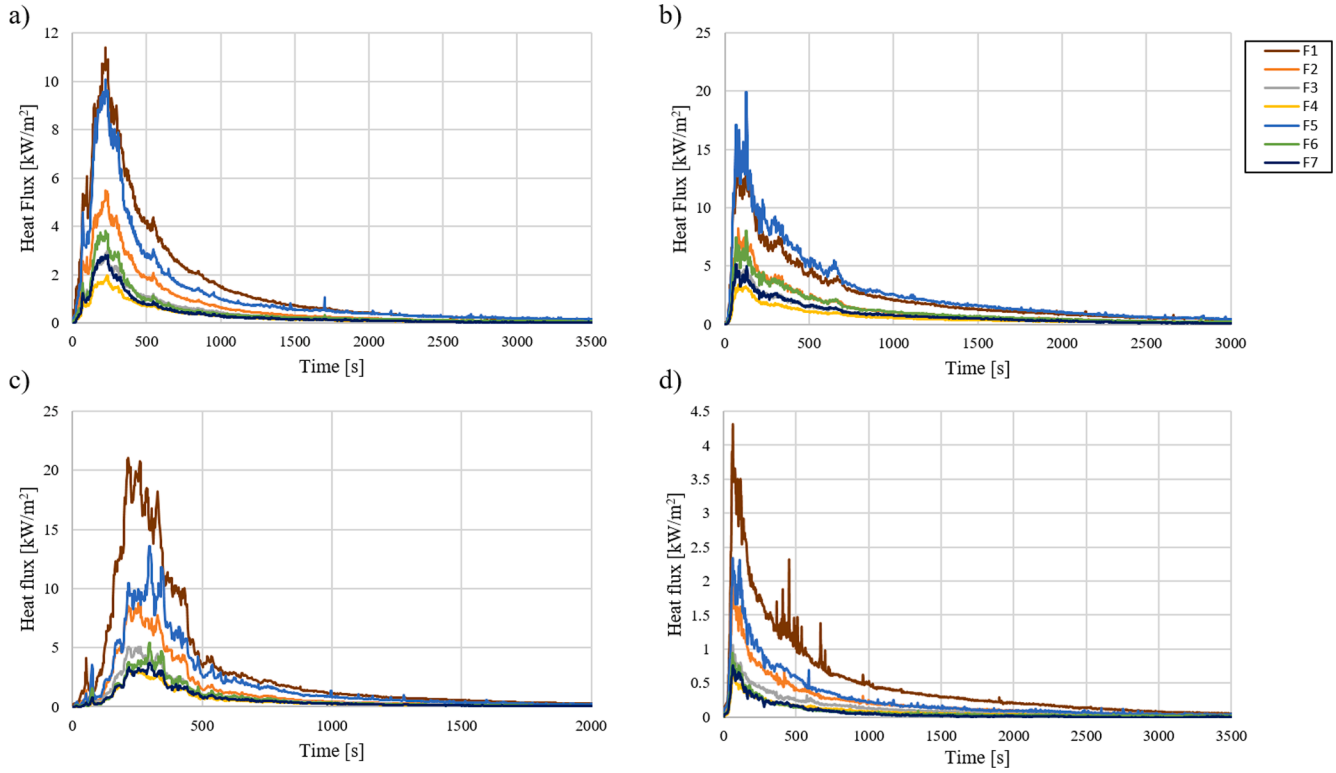

Fig. 12. Recorded heat fluxes for: a) test 1, b) test 2, c) test 3 and d) test 4.

Table 5
Radiative heat flux for each test at a distance of 1.5 m from the fuel pack.

	L[m]	D[m]	H[m]	φ	T_f[K]	$\dot{q}_f''$[kW/m^2]
Test 1	2.47	1.94	1.80	0.17	888	5.9
Test 2	2.28	1.56	2.90	0.16	1047	11.0
Test 3	2.36	1.71	3.48	0.17	931	7.4
Test 4	1.90	0.80	1.2	0.08	947	3.5

Table 6
Average and maximum flame heights for each test.

Test	Number of frames (images)	Average flame height [m]	Maximum flame height [m]	Time at which maximum flame height is reached [s]
Test 1	516	1.22	2.65	170
Test 2	645	1.47	3.23	134
Test 3	1564	1.61	3.60	271
Test 4	509	1.05	2.64	67

result to be those with the highest gross heat of content, since these are some of the items with the highest mass and highest material gross heat of combustion, with 46.37 MJ/kg and 39.3 MJ/kg respectively (Babrauskas, 1991). These are the items that drive the combustion, and are therefore the most hazardous ones, in the fuel packs in tests 1 and 2, which contain a bigger variety of materials compared to the other two packs. The toy house in the first test and the oil-based paint in the second one account for respectively 36% and 76% of the total gross heat content of the fuel packs. The total approximate gross heat content for each fuel pack was calculated as 1807 MJ for test 1, 4505 MJ for test 2, 1916 MJ for test 3 and 1460 MJ for test 4. Also in this case the fuel pack of test 2 is the most hazardous one, with a much higher gross heat content compared to the others. The fuel packs of the other three tests present close values when it comes to their gross heat content, still showing however the one in test 3 as the second hazardous one, and the one of test 4 as the least hazardous. The absorption of the paint by the sand placed to protect the scale and the subsequent fact that a big portion of the paint was not exposed to the air might explain why test 4 showed the lowest HRR and mass loss, especially since its calculated gross heat content is much higher than the effective fire load. Part of the paint in test 2 was also absorbed by the sand, while part of it spilled on top of the other items, remaining therefore exposed to the air.

Also the obtained fire growth rate reiterates that the fuel pack of test 2 is the most hazardous one, given that it will reach its peak HRR very rapidly (within about 3 min). All fuel packs however reach their peak HRR within 5 min from ignition, giving very little time for firefighting intervention to avoid that the fires will reach their peak values. Potential fire spread through a property could also be a consequence of late intervention, since the obtained peak flame heights for each test are high enough to potentially provide ignition due to direct flame impingement of fuels located above the fuel packs (e.g. trees, fuels located on higher

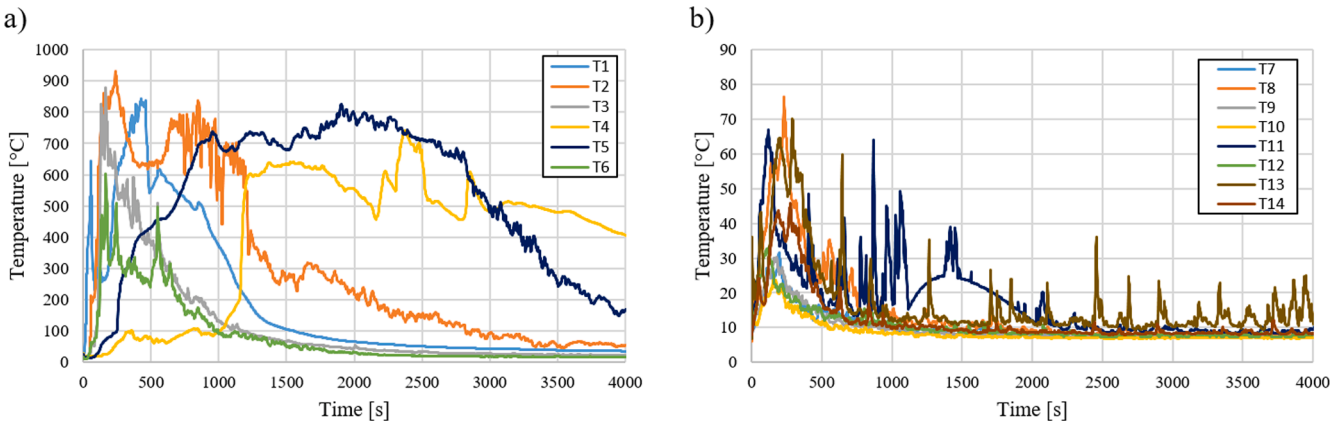

Fig. 13. Temperatures for test 1: a) flame and b) air.

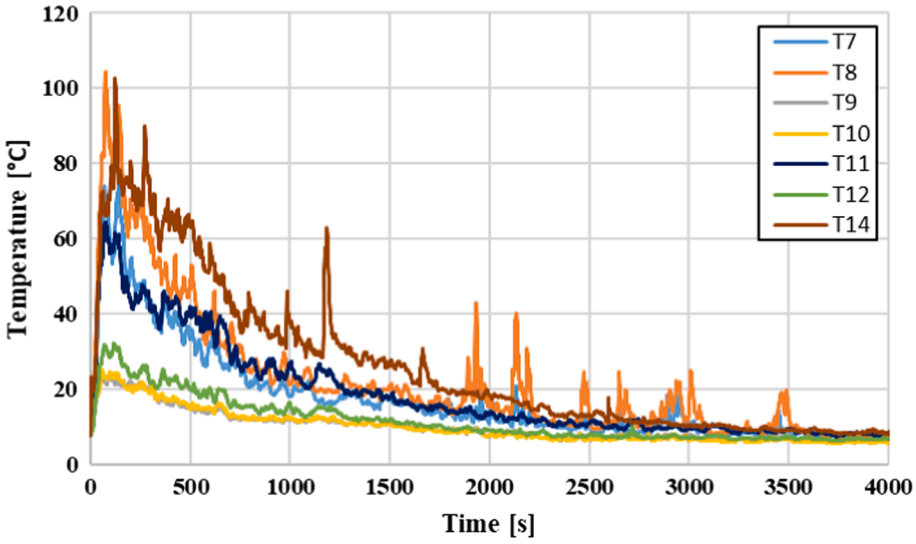

Fig. 14. Air temperatures for test 2.

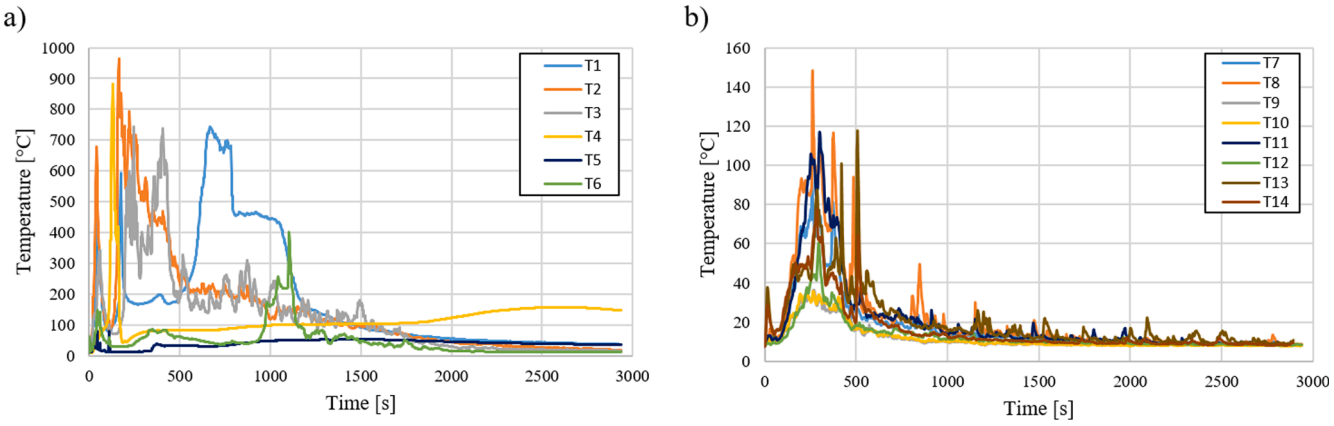

Fig. 15. Temperatures for test 3: a) flame and b) air.

floors of a structure, etc.). This can allow fire spread through other elements on a property even when the wildfire has already passed through, especially taking the long period of time for the combustion of these fuels into account. The melting of the plastic items and the pouring out of the paint from the buckets could also cause fire spread through other elements located on a property, since it increased the surface of the fire by almost doubling its width for all fuel packs. This creates a risk for the ignition of other items located at further distances from the fuel packs. The spacing between these types of fuels and others present on the property should consider this flaming surface expansion in order to avoid fire spread through a property. In addition, the paint in fuel packs 2 and 4 was partly absorbed by the sand placed to protect the scale. On

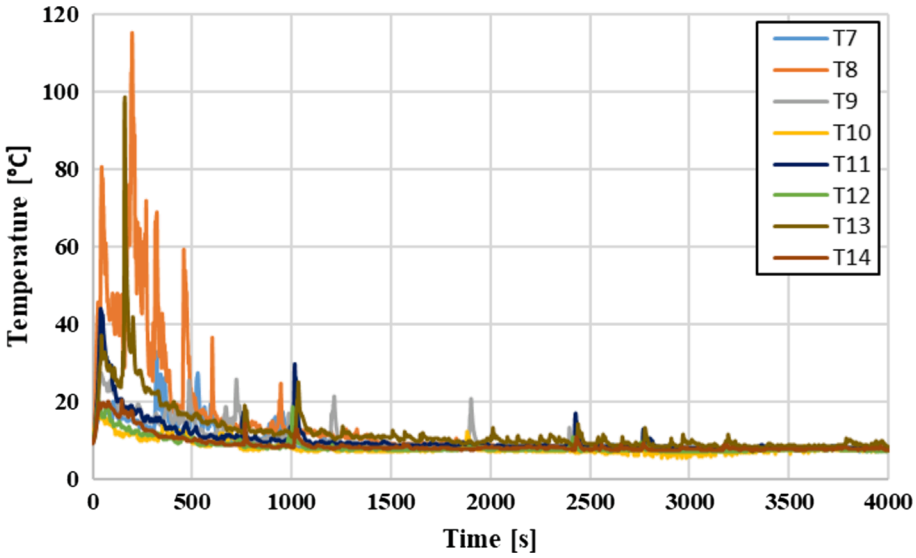

Fig. 16. Air temperatures for test 4.

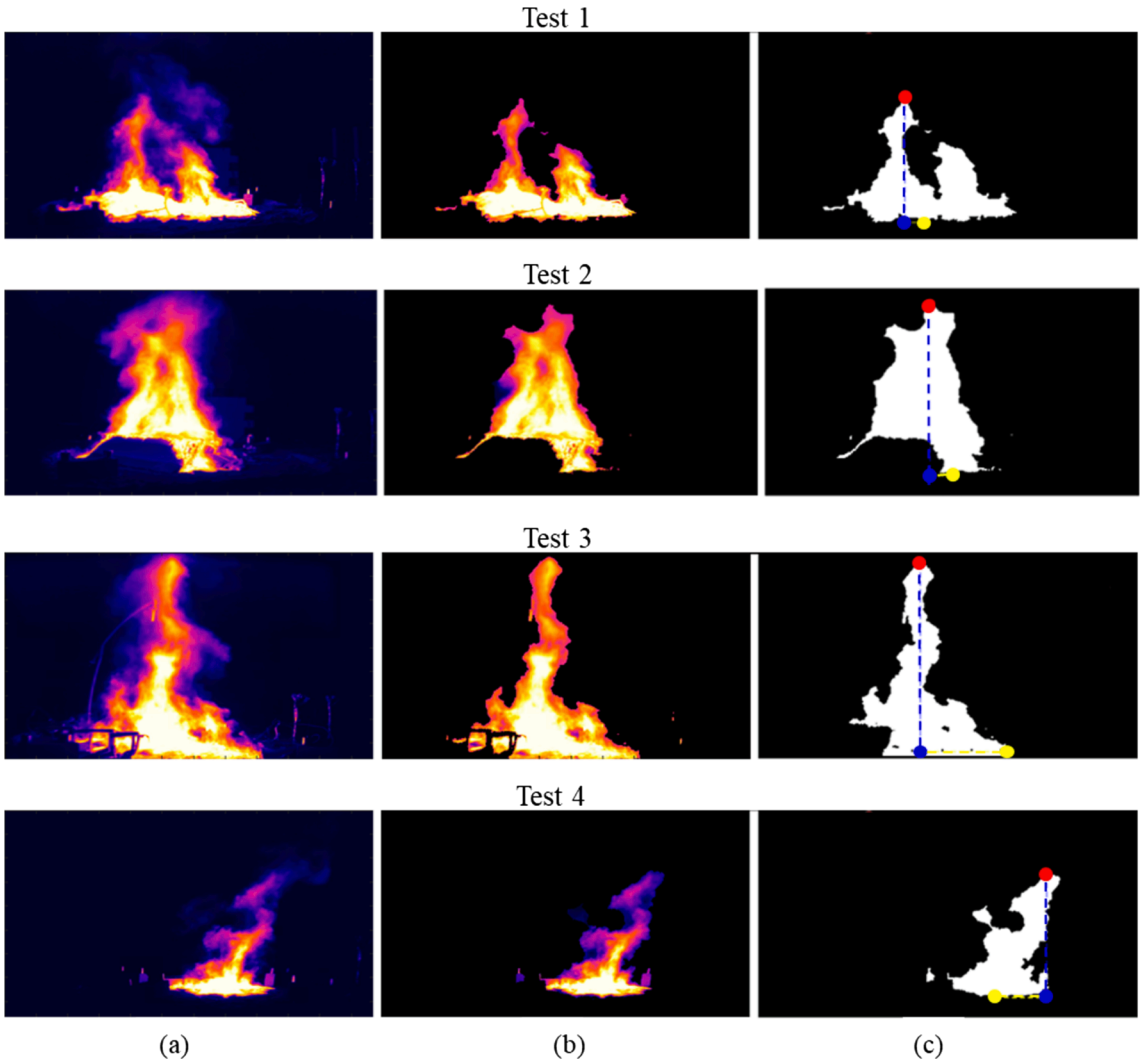

Fig. 17. Example of the results obtained from: (a) an original IR frame, (b) the segmented image and (c) the calculation of the corresponding flame height for test 1 at 219 s, test 2 at 90 s, test 3 at 194 s and test 4 at 88 s. The yellow and red dots indicate the lowest and highest pixels, while the blue dot is the horizontal projection of the lowest pixel. The dashed line between the red and blue dot gives the flame height. (For interpretation of the references to colour in this figure legend, the reader is referred to the web version of this article.)

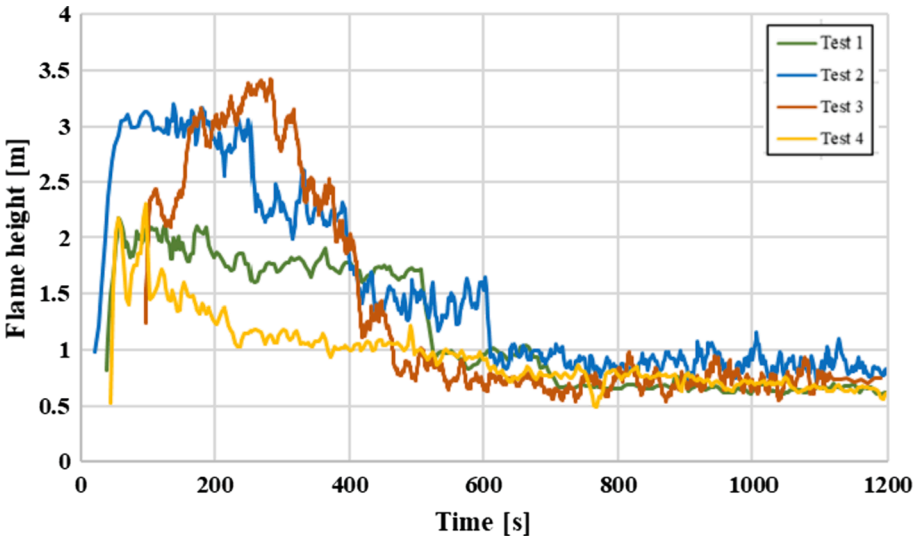

Fig. 18. Flame height for the first 20 min of each test, averaged every 10 s.

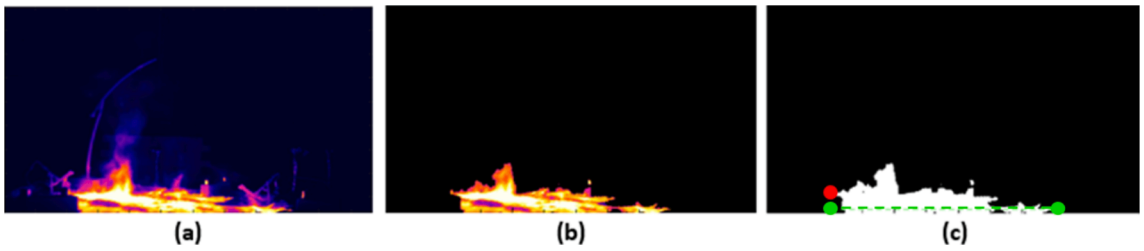

Fig. 19. Example of the results obtained from: (a) an original IR frame, (b) the segmented image and (c) the calculation of the corresponding fire width for test 3 at 621 s.

Table 7
Safe distance for each test.

	L[m]	φ	Safe distance from fuel pack [m]
Test 1	4.14	0.07	3.2
Test 2	6.24	0.04	5.5
Test 3	5.39	0.06	4.5
Test 4	2.35	0.05	2.0

other types of surfaces, the paint would expand even more, creating an even bigger flaming surface.

Safety distances must not only be respected in order to avoid fire spread through a property, but also to protect the people present on the property from the radiant heat of these fuel packs. The tenability limit for exposure of skin to radiant heat is approximately 2.5 kW/m^2; radiant heat at this level and above causes skin pain followed by burns within a few seconds (Purser, 2000). According to the values in Table 5, a person standing at a distance of 1.5 m from the analysed fuel packs will feel pain if not protected with appropriate protective clothing. The safe distance for each fuel pack (calculated with Eqs. (1) and (2)), at which the radiative heat flux is below 2.5 kW/m^2, is given in Table 7.

When looking at the smoke concentrations, the combustion of none of the fuel packs leads to incapacitation or death, given that the concentration of CO_2 remained well below 5%, and the one of CO never reached 30,000 ppm/min (Hurley et al., 2016), corresponding to a well-ventilated scenario, which is expected at the WUI. Other toxic combustion products such as HCN and HCl were not measured, although these can also pose a hazard to people located near the burning fuels.

The combustion of these fuel packs also has the potential to cause structural damage. Should it happen in smaller spaces, such as the semi-confined spaces in Fig. 1 and Fig. 2, then a hot smoke layer would form and the heat produced by the combustion would accumulate inside these spaces. This could lead to structural damage of the envelope of these constructions, along with higher temperatures and heat fluxes due to the radiation of the hot smoke layer. The combustion of these fuels, if located close to glazing systems, can also cause cracking and falling of the glass (Babrauskas, 2011), along with melting of the frame, should this be composed of plastic materials such as PVC. In its large scale experiments, Mowrer (1998) analysed window breakage induced by exterior fires, and in his large scale tests he found that single pane float glass window with a vinyl frame cracked when exposed to a heat flux of 9 kW/m^2. The peak heat fluxes registered for the first three tests go above this value, meaning that a window placed at 1.5 m from the fuel packs of these tests, if not protected (e.g. shutters), would eventually fail. This will allow the entrance of firebrand or flames into the building, which can then cause the ignition of the items located in its interior.

The data gathered in these tests are very useful as inputs for CFD simulations that include these WUI microscale scenarios, so that results can be compared to performance criteria for the evaluation of the hazard caused by the combustion of these fuel packs.

4. Conclusions

The combustion of four different fuel packs containing items that can be present on properties at the WUI is investigated in order to obtain quantitative information on the burning behaviour of these types of fuel. Data on HRR, MLR, fire load, smoke concentrations, temperatures and heat fluxes were recorded for each test. The fuel packs that showed higher peak values, and are thus more hazardous, are the one containing garden furniture and the one with pallets, cardboard, paint and foam

mats. However, all fuel packs showed significant peak flame heights along with a doubling in their width, meaning that the flaming area expanded significantly during the combustion. This will allow for unforeseen fire spread through a property even after the passage of the wildfire front. All fuel packs also gave radiative heat flux values higher than the tenability limit for exposure of skin to radiant heat within 1.5 m form the burning items. Safe distances up to 5.5 m have been calculated.

The obtained data can be used as input for PBD methodologies for the quantification of hazards and vulnerabilities of WUI microscale scenarios, in order to expand the current knowledge of the defensible space in these environments. This way it will be possible to analyse specific scenarios such as those involving particular structural elements (e.g. semi-confined spaces, windows), which have been identified in past fires as possible pathways to the ignition and destruction of structures at the WUI microscale.

Author contribution

Conceptualization and methodology, Elsa Pastor, Eulàlia Planas, Frederic Heymes, Pascale Vacca; software, Christian Mata; validation, Eulàlia Planas, Elsa Pastor; resources, Frederic Heymes, Eulàlia Planas, Elsa Pastor; data curation, Pascale Vacca, Juan Antonio Muñoz; writing – original draft preparation, Pascale Vacca; project administration, Elsa Pastor; funding acquisition, Eulàlia Planas, Elsa Pastor; All authors have read and agreed to the published version of the manuscript.

Declaration of Competing Interest

The authors declare that they have no known competing financial interests or personal relationships that could have appeared to influence the work reported in this paper.

Acknowledgments

This research was partially funded by the European Union Civil Protection (Project GA 826522 WUIVIEW UCPM-2018-PP-AG), the Spanish Ministry of Economy and Competitiveness (Project CTQ2017-85990-R, co-financed with FEDER funds) and the Autonomous Government of Catalonia (project no. 2017-SGR-392).

References

Babrauskas, V., 2011. Glass breakage in fires. Fire Sci. Technol. Inc. 1–7.
Babrauskas, V., 1991. Tables and Charts. In: Cote, A.E., Linville, J. (Eds.), Fire Protection Handbook. National Fire Protection Association.
Caballero, D., Sjöström, J., 2019. Deliverable D5.1 - Inventory of pattern scenarios.
Caton, S.E., Hakes, R.S.P., Gorham, D.J., Zhou, A., Gollner, M.J., 2017. Review of Pathways for Building Fire Spread in the Wildland Urban Interface Part I: Exposure Conditions. Fire Technol. 53, 429–473. https://doi.org/10.1007/s10694-016-0589-z.
Chan, T., Vese, L., 1999. An Active Contour Model without Edges. In: International Conference on Scale-Space Theories in Computer Vision. Springer, Berlin, Heidelberg. https://doi.org/10.1007/3-540-48236-9_13.
Cohen, J., 2010. The wildland-urban interface fire problem. Fremontia.
Cohen, J.D., 2000. Preventing Disaster: Home Ignitability in the Wildland-Urban Interface. J. For. 98, 15–21.
Fontana, M., Kohler, J., Fischer, K., De Sanctis, G., 2016. In: SFPE Handbook of Fire Protection Engineering. Springer New York, New York, NY, pp. 1131–1142. https://doi.org/10.1007/978-1-4939-2565-0_35.
Hakes, R.S.P., Caton, S.E., Gorham, D.J., Gollner, M.J., 2017. A Review of Pathways for Building Fire Spread in the Wildland Urban Interface Part II: Response of Components and Systems and Mitigation Strategies in the United States. Fire Technol. 53 (2), 475–515. https://doi.org/10.1007/s10694-016-0601-7.
Heskestad, G., 1982. Engineering Relations for Fire Plumes. In: SFPE TR. MA, USA, Boston, pp. 82–88.
Hurley, M.J., Gottuk, D., Hall, J.R., Harada, K., Kuligowski, E., Puchovsky, M., Torero, J., Watts, J.M., Wieczorek, C. (Eds.), 2016. SFPE Handbook of Fire Protection Engineering. Springer New York, New York, NY.
Janssens, M., 2016. In: SFPE Handbook of Fire Protection Engineering. Springer New York, New York, NY, pp. 905–951. https://doi.org/10.1007/978-1-4939-2565-0_27.
Manzello, S.L., Blanchi, R., Gollner, M.J., Gorham, D., McAllister, S., Pastor, E., Planas, E., Reszka, P., Suzuki, S., 2018. Summary of workshop large outdoor fires and the built environment. Fire Saf. J. 100, 76–92. https://doi.org/10.1016/j.firesaf.2018.07.002.
Mata, C., Pastor, E., Rengel, B., Valero, M., Planas, E., Palacios, A., Casal, J., 2018. Infrared Imaging Software for Jet Fire Analysis. Chem. Eng. Trans. 2283–9216. 10.3303/CET1867147.
Mell, W.E., Manzello, S.L., Maranghides, A., Butry, D., Rehm, R.G., 2010. The wildland-urban interface fire problem - Current approaches and research needs. Int. J. Wildl. Fire 19 (2), 238. https://doi.org/10.1071/WF07131.
Mowrer, F.W., 1998. Window breakage induced by exterior fires. Second International Conference on Fire.
National Fire Protection Association, 1985. Guide for Smoke and Heat Venting, NFPA 204M.
National Fire Research Laboratory, 2020. Fire Calorimetry Database (FCD) [WWW Document]. https://doi.org/https://doi.org/10.18434/mds2-2314.
Pastor, E., Muñoz, J.A., Caballero, D., Àgueda, A., Dalmau, F., Planas, E., 2019. Wildland-Urban Interface Fires in Spain: Summary of the Policy Framework and Recommendations for Improvement. Fire Technol. https://doi.org/10.1007/s10694-019-00883-z.
Purser, D.A., 2000. Toxic product yields and hazard assessment for fully enclosed design fires. Polym. Int. 49, 1232–1255. https://doi.org/10.1002/1097-0126(200010)49:10<1232::AID-PI543>3.0.CO;2-T.
Ricci, F., Scarponi, G.E., Pastor, E., Planas, E., Cozzani, V., 2021. Safety distances for storage tanks to prevent fire damage in Wildland-Industrial Interface. Process Saf. Environ. Prot. 147, 693–702. https://doi.org/10.1016/j.psep.2021.01.002.
Ronchi, E., Gwynne, S.M.V., Rein, G., Intini, P., Wadhwani, R., 2019. An open multi-physics framework for modelling wildland-urban interface fire evacuations. Saf. Sci. 118, 868–880. https://doi.org/10.1016/j.ssci.2019.06.009.
Scarponi, G.E., Pastor, E., Planas, E., Cozzani, V., 2020. Analysis of the impact of wildland-urban-interface fires on LPG domestic tanks. Saf. Sci. 124, 104588. https://doi.org/10.1016/j.ssci.2019.104588.
Shokri, M., Beyler, C.L., 1989. Radiation from Large Pool Fires. J. Fire Prot. Eng. 1 (4), 141–149. https://doi.org/10.1177/104239158900100404.
Vacca, P., Caballero, D., Pastor, E., Planas, E., 2020. WUI fire risk mitigation in Europe: A performance-based design approach at home-owner level. J. Saf. Sci. Resil. 1 (2), 97–105. https://doi.org/10.1016/j.jnlssr.2020.08.001.